J|A|C|S
ARTICLES
Published on Web 10/18/2002

Electroluminescence in Ruthenium(II) Complexes

Stefan Bernhard,[†] Jason A. Barron,[†] Paul L. Houston,[†] Héctor D. Abruña,[†] Jennifer L. Ruglovksy,[‡] Xicun Gao,[‡] and George G. Malliaras*[,‡]

Contribution from the Department of Chemistry and Chemical Biology, Baker Lab, Cornell University, Ithaca, New York 14853-1301 and Department of Materials Science and Engineering, Cornell University, Ithaca, New York 14853-1501

Received May 25, 2002

Abstract: We have investigated the electrochemical, spectroscopic, and electroluminescent properties of a family of diimine complexes of Ru featuring various aliphatic side chains as well as a more extended π-conjugated system. The performance of solid-state electroluminescent devices fabricated from these complexes using indium tin oxide (ITO) and gold contacts appears to be dominated by ionic space charge effects. Their electroluminescence efficiency was limited by the photoluminescence efficiency of the Ru films and not by charge injection from the contacts. The incorporation of di-*tert*-butyl side chains on the dipyridyl ligand was found to be the most beneficial substitution in terms of reducing self-quenching of luminescence.

Introduction

Transition metal complexes have recently emerged as some of the most promising materials for efficient solid-state electroluminescent materials.[1−21] Motivated by the high efficiencies achieved in solution (which approach 25%),[22] a variety of small molecules and polymers have been synthesized and evaluated in solid-state electroluminescent devices. Early attempts led to efficiencies that were fairly low, typically below 0.1%.[1−5] Recently, however, Handy et al.[6,10] showed that efficiencies of the order of 1% can be achieved in single layer devices made from $[Ru(bpy)_3]^{2+}$, where bpy is 2,2′-bipyridine. Further progress was achieved by dilution of this material into polymer matrices, which led to devices with efficiencies of up to 3%,[18,19] approaching the photoluminescence efficiency.

The mechanism of operation of these devices differs from that of traditional organic light emitting diodes and is similar to that in electrochemical cells.[23−25] $[Ru(bpy)_3]^{2+}$ and related complexes carry a net 2+ charge and are compensated by negative counterions such as PF_6^-. The accumulation of these counterions near the anode (and the corresponding depletion near the cathode) enhances hole and electron injection, respectively. As a result, efficient devices can be made with air stable electrodes, in contrast to conventional organic light emitting diodes that require low work function cathodes. The penalty comes in terms of a turn-on time, which is determined by the ionic mobility. However, with the judicious choice of the counterions or by using pulsing schemes, this time can be reduced to a few seconds.[10,19]

Clearly, more thorough studies are needed to establish the relationship between the chemical structure of these complexes and their electroluminescent properties. One of the most important tradeoffs in the field of organic electroluminescence is that between transport and emission.[26] Simply stated, the proximity of chromophores (which is important for efficient charge transport) often causes quenching of their luminescence. Although this tradeoff can be largely alleviated by multilayer structures or dye doping (see ref 25), it is important to explore

* Corresponding author: Materials Science and Engineering, Cornell University, 327 Bard Hall, Ithaca, NY 14853-1501. Telephone: (607) 255-19516. Fax: (607) 255-2365. E-mail: george@ccmr.cornell.edu.
[†] Department of Chemistry and Chemical Biology, Cornell University.
[‡] Department of Materials Science and Engineering, Cornell University.

(1) Lee, J.-K.; Yoo, D. S.; Handy, E. S.; Rubner, M. F. *Appl. Phys. Lett.* **1996**, *69*, 1686.
(2) Maness, K. M.; Terrill, R. H.; Meyer, T. J.; Murray, R. W.; Wightman, R. M. *J. Am. Chem. Soc.* **1996**, *118*, 10609.
(3) Lee, J.-K.; Yoo, D.; Rubner, M. F. *Chem. Mater.* **1997**, *9*, 1710.
(4) Yoo, D.; Wu, A.; Lee, J.; Rubner, M. F. *Synth. Met.* **1997**, *85*, 1425.
(5) Maness, K. M.; Masui, H.; Wightman, R. M.; Murray, R. W. *J. Am. Chem. Soc.* **1997**, *119*, 3987.
(6) Handy, E. S.; Abbas, E. D.; Pal, A. J.; Rubner, M. F. *Proc. SPIE-Int. Soc. Opt. Eng.* **1998**, *3476*, 62.
(7) Elliot, C. M.; Pichot, F.; Bloom, C. J.; Rider, L. S. *J. Am. Chem. Soc.* **1998**, *120*, 6781.
(8) Wu, A.; Lee, J.; Rubner, M. F. *Thin Solid Films* **1998**, *327−329*, 663.
(9) Lyons, H.; Abbas, E. D.; Lee, J.-K.; Rubner, M. F. *J. Am. Chem. Soc.* **1998**, *120*, 12100.
(10) Handy, E. S.; Pal, A. J.; Rubner, M. F. *J. Am. Chem. Soc.* **1999**, *121*, 3525.
(11) Wu, A.; Yoo, D.; Lee, J.-K.; Rubner, M. F. *J. Am. Chem. Soc.* **1999**, *121*, 4883.
(12) Collinson, M. M.; Taussig, J.; Martin, S. A. *Chem. Mater.* **1999**, *11*, 2594.
(13) Collinson, M. M.; Martin, S. A. *Chem. Commun.* **1999**, *899−900*, 899.
(14) Ng, W. Y.; Gong, X.; Chan, W. K. *Chem. Mater.* **1999**, *11*, 1165.
(15) Chan, W. K.; Ng, P. K.; Gong, X.; Hou, S. *J. Mater. Chem.* **1999**, *9*, 2103.
(16) Rudmann, H.; Kaplan, L.; Sevian, H.; Rubner, M. F. *Polym. Mater. Sci. Eng.* **2000**, *83*, 235.
(17) Gao, F. G.; Bard, A. J. *J. Am. Chem. Soc.* **2000**, *122*, 7426.
(18) Rudmann, H.; Rubner, M. F. *J. Appl. Phys.* **2001**, *90*, 4338.
(19) Rudmann, H.; Shimada, S.; Rubner, M. F. *J. Am. Chem. Soc.* **2002**, *124*, 4918.
(20) Buda, M.; Kalyuzhny, G.; Bard, A. J. *J. Am. Chem. Soc.* **2002**, *124*, 6090.
(21) Bernhard, S.; Gao, X.; Abruña, H. D.; Malliaras, G. G. *Adv. Mater.* **2002**, *14*, 433.
(22) McCord, P.; Bard, A. J. *J. Electoanal. Chem.* **1991**, *318*, 91.
(23) Pei, Q. B.; Yu, G.; Zhang, C.; Heeger, A. J. *Science* **1995**, *269*, 1086.
(24) deMello, J. C.; Tessler, N.; Graham, S. C.; Friend, R. H. *Phys. Rev. B* **1998**, *57*, 12951.
(25) Pichot, F.; Bloom, C. J.; Rider, L. S.; Elliott, C. M. *J. Phys. Chem. B* **1998**, *102*, 3523.
(26) Scott, J. C.; Malliaras, G. G. *Conjugated Polymers*; Hadziioannou, G., van Hutten, P. F., Eds.; Wiley-VCH: New York, 1999; Chapter 13.

10.1021/ja0270524 CCC: $22.00

the intrinsic electroluminescent properties of the chromophores. With this in mind, the properties of a family of diimine complexes of Ru with ligands featuring various aliphatic side chains as well as a more extended π-conjugated ligand have been examined. Their electrochemical and optical properties were measured and correlated to their device characteristics.

Experimental Section

General. Solvents and reagents for synthesis were purchased from Aldrich and used without further purification. Acetonitrile (Burdick and Jackson; distilled in glass) for electrochemical experiments was dried over 4-Å molecular sieves for at least 48 h. Tetra-*n*-butylammonium hexafluorophosphate (TBAH) (GFS Chemicals) was recrystallized 3 times from ethyl acetate and dried under vacuum for 96 h. $[Ru(bpy)_3]^{2+}(PF_6^-)_2$ (bpy = 2,2′-bipyridine) and $[Ru(phen)_3]^{2+}(PF_6^-)_2$ (phen = 1,10-phenanthroline) were prepared according to the procedure published by Cooley et al.[27] ESIMS and EIMS spectra were obtained on a Micromass Quattro I triple quadrupole tandem mass spectrometer, and a Varian Inova-400 spectrometer was used to collect ^{1}H and ^{13}C NMR data.

Synthesis. A. 4,4′-Di-*n*-pentyl-2,2′-dipyridyl (1). A solution of 4,4′-dimethyl-2,2′-dipyridyl (0.92 g, 5.0 mmol) in 50 mL of dry THF was cooled to −40 °C, and a solution of lithium diisopropylamide (5.5 mL, 2 M, 11.0 mmol) was added via a syringe under nitrogen. The resulting deep blue solution was allowed to warm to −5 °C and kept at this temperature for 1 h. After the solution was cooled to −20 °C, 1-bromobutane (1.51 g, 1.18 mL, 11 mmol) was added to the reaction mixture, which was then left to warm to 0 °C. After 2 h, the blue mixture became light brown and a sample of the reaction mixture was analyzed via thin-layer chromatography (alumina−hexane/ethyl acetate/triethylamine 150:30:1), revealing a mixture of mono- and di-substituted products. Further addition of lithium diisopropylamide (3.0 mL, 2 M, 6.0 mmol) at 0 °C and the addition of 1-bromobutane (0.82 g, 0.64 mL, 6 mmol) after 30 min lead to an increase of the disubstituted product. The repetition of this alkylation step (lithium diisopropylamide (2.5 mL, 2 M, 5.0 mmol) and 1-bromobutane (0.68 g, 0.54 mL, 5 mmol)) produced over 75% of 4,4′-di-*n*-pentyl-2,2′-dipyridyl. The reaction mixture was quenched with ammonium chloride solution (100 mL, 5%) and extracted with CH_2Cl_2 (3 × 100 mL). The combined organic layers were washed with water (100 mL) and, to remove the monoalkylated product, extracted with 3 × 100 mL HCl (1:10). The organic phase was extracted 3 times with HCl (1:1), and the combined aqueous layers were washed with dichloromethane. The bypyridine was separated from the aqueous phase through neutralization with Na_2CO_3 and a subsequent extraction with hexane (3 × 200 mL). The combined organic phases were dried ($MgSO_4$), and the solvent was evaporated to yield a slowly crystallizing colorless solid. Yield: 0.85 g (2.86 mmol, 57%). Analytical Data: ^{1}H NMR ($CDCl_3$, 400 MHz) δ 8.52 (1H, d, J = 4.9), 8.19 (1H, d, J = 1.0), 7.10 (1H, dd, J = 4.9, J = 1.3), 2.65 (2H, t, J = 7.3), 1.67 (2H, m), 1.31 (4H, m), 0.86 (3H, m). EIMS (m/z) 296.2 (10%, $[M^+]$), 267.2 (5%, $[M-C_2H_5]^+$), 253.2 (35%, $[M-C_3H_7]^+$), 240.2 (100%, $[M-C_4H_8]^+$).

B. $[Ru(1)_3]^{2+}(PF_6^-)_2$. A mixture of 4,4′-di-*n*-pentyl-2,2′-dipyridyl (**1**) (0.326 g, 1.1 mmol) and ruthenium(III) chloride (0.069 g, 0.33 mmol) in 10 mL 1,2-ethanediol was refluxed in a microwave oven for 16 min.[28] Methanol (100 mL) and water (30 mL) were added to the reaction mixture, and the excess ligand in the orange solution was removed through an extraction with hexane (5 × 50 mL). A solution of 2.0 g of NH_4PF_6 dissolved in water/methanol (10:3) was added, resulting in the precipitation of the complex, which was filtered, rinsed with water, and subsequently dried. Yield: 0.35 g (0.27 mmol, 82%). Analytical Data: ^{1}H NMR (d_6-Acetone, 400 MHz) δ 8.70 (1H, d, J = 1.5), 7.81 (1H, d, J = 5.9), 7.39 (1H, dd, J = 5.9, J = 1.1), 2.83 (2H, t, J = 7.8), 1.6−1.9 (2H, m), 1.2−1.4 (4H, m), 0.8 (3H, m). ESIMS (m/z) 495.7 (100%, $[M^{2+}]$).

C. $[Ru(bpy)_2(1)]^{2+}(PF_6^-)_2$. A mixture of 4,4′-di-*n*-pentyl-2,2′-dipyridyl (**1**) (0.326 g, 1.1 mmol) and *cis*-bis(2,2′-bipyridine)dichlororuthenium(II) hydrate[29] (0.484 g, 1.0 mmol) in 10 mL of 1,2-ethanediol was refluxed in a microwave oven for 16 min.[28] Water (150 mL) was added to the reaction mixture, and the excess ligand in the orange solution was removed through an extraction with ether (5 × 50 mL). A solution of 2.0 g of NH_4PF_6 dissolved in water was added to precipitate the complex, which was subsequently filtered off, rinsed with water, and dried. Yield: 0.78 g (0.78 mmol, 78%). Analytical Data: ^{1}H NMR (d_6-Acetone, 400 MHz) δ 8.78 (2H, d, J = 6.3), 8.72 (1H, d, J = 1.0), 8.2 (H, m), 8.02 (2H, d, J = 4.9), 7.85 (1H, d, J = 5.4), 7.52 (2H, m), 7.41 (2H, dd, J = 5.8, J = 1.5), 2.82 (2H, t, J = 8.3), 1.6−1.7 (2H, m), 1.2−1.4 (4H, m), 0.8 (3H, m). ESIMS (m/z) 355.6 (100%, $[M^{2+}]$).

D. $[Ru(m\text{-}bpy)_3]^{2+}(PF_6^-)_2$. A mixture of 4-methyl-2,2′-dipyridyl (0.536 g, 3.15 mmol) and ruthenium(III) chloride hydrate (0.207 g, 1.0 mmol) in 10 mL of 1,2-ethanediol was refluxed in a microwave oven for 16 min. Water (150 mL) was added to the reaction mixture, and the excess ligand in the orange solution was removed through an extraction with ether (5 × 50 mL). A solution of 2.0 g of NH_4PF_6 dissolved in water was added, and the formed precipitate was filtered off, rinsed with water, and dried. The complex was purified through vapor diffusion crystallization with acetonitrile/diethyl ether. Yield: 0.77 g (0.85 mmol, 85%). Analytical Data: ^{1}H NMR (d_6-Acetone, 400 MHz) δ 8.8−8.7 (1H, m), 8.7−8.63 (1H, m), 8.2−8.1 (1H, m), 8.03−7.94 (1H, m), 7.85−7.75 (1H, m), 7.52 (1H, bs), 7.38 (1H, bs), 2.52 (3H, bs). ESIMS (m/z) 306 (100%, $[M^{2+}]$).

E. $[Ru(dtb\text{-}bpy)_3]^{2+}(PF_6^-)_2$. $[Ru(4,4′\text{-di-}tert\text{-butyl-}2,2′\text{-dipyridyl})_3]^{2+}$ was prepared employing a procedure identical to the one described above for $[Ru(m\text{-}bpy)_3]^{2+}$. Analytical Data: ^{1}H NMR (d_6-Acetone, 400 MHz) δ 8.8−8.7 (1H, m), 8.84 (1H, d, J = 2.0), 7.80 (1H, d, J = 6.0), 7.54 (1H, dd, J = 2.4, J = 5.6), 1.38 (9H, bs). ESIMS (m/z) 453.3 (100%, $[M^{2+}]$).

Characterization. Electrochemical experiments were carried out with a BAS CV-27 potentiostat. Three compartment electrochemical cells (separated by medium porosity sintered glass disks) with the provision for gas addition were employed. All joints were standard-taper, so that all compartments could be hermetically sealed with Teflon adapters. A platinum disk (geometric area = 0.008 cm^2) was used as a working electrode. The electrode was polished prior to use with 1-μm diamond paste (Buehler) and rinsed thoroughly with water and acetone. A large area platinum wire coil was used as a counter electrode. All potentials are referenced to a saturated Ag/AgCl electrode without regard for the liquid junction potential.

UV−vis absorption spectra were recorded using a Hewlett-Packard 8453 diode-array spectrometer. Fluorescence spectra were obtained using a SPEX 1681 Minimate-2 spectrofluorimeter with a Spectra Acq CPU controller. The excitation wavelength for all photoluminescence (PL) measurements was 450 nm. All spectra were acquired normal to the incident beam. Solution spectra were measured in acetonitrile (Mallinckrodt, HPLC grade) at a concentration of 0.01 mM. The PL intensity was measured for a solution of an absorbance of 0.15 at 450 nm and was used to calculate the quantum efficiency, using as a reference the literature value of 6.1% for $[Ru(bpy)_3]^{2+}$ in acetonitrile.[30] Spin-coated films on quartz slides were employed to obtain the solid-state PL characteristics at an angle of incidence of 45°.

For the fabrication of the light emitting devices, films were spin coated from an acetonitrile solution onto glass substrates covered with prepatterned ITO electrodes (Thin Film Devices, Anaheim, CA). The thicknesses of the films were around 75 nm, measured with profilo-

(27) Cooley, L. F.; Headford, C. E. L.; Elliot, C. M.; Kelley, D. F. *J. Am. Chem. Soc.* **1988**, *110*, 6673−6682.
(28) Mingos, D. M. P.; Baghurst, D. R. *J. Organomet. Chem.* **1990**, *348*, C57.
(29) Sullivan, B. P.; Salmon, D. J.; Meyer, T. J. *Inorg. Chem.* **1978**, *17*, 3334.
(30) Kalyanasundaram, K. *Photochemistry of Polypyridine and Porphyrin Complexes*; Academic Press: London, 1992.

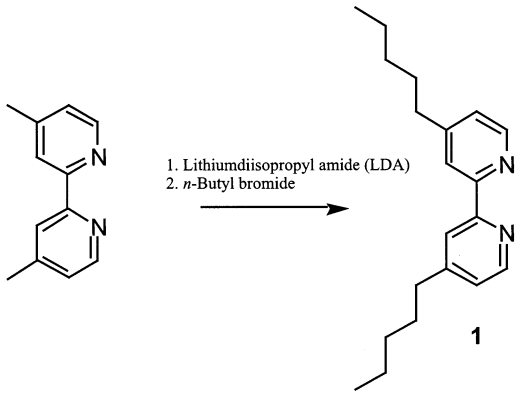

Figure 1. Synthetic pathway for the preparation of 4,4′-di-*n*-pentyl-2,2′-dipyridyl (**1**).

metry. The ITO substrates were cleaned just before the deposition of the organic layer by a deionized water bath, followed by a UV/ozone treatment. The films were dried for 12 h at 100 °C under vacuum and were introduced in a dry nitrogen glovebox for further processing and characterization. 200-Å thick Au cathodes were deposited through a shadow mask that defined six devices per substrate with a 3 mm^2 active area each. The deposition was carried out in an intermittent way in order to minimize heating of the organic film. The electrical characteristics of the devices were measured with a Keithley 236 source-measure unit (with the ITO electrode wired as the anode, unless otherwise stated), and the radiance, with a calibrated UDT S370 optometer, coupled to an integrating sphere. The electroluminescence spectra were measured with a calibrated S2000 Ocean Optics fiber spectrometer. The emission was found to be uniform throughout the area of each device.

Results and Discussion

The frequently utilized pathway employing lithium diisopropylamide as a base for the monoalkylation of 4-methyl substituted pyridines was used to prepare 4,4′-di-*n*-pentyl-2,2′-dipyridyl (**1**) (Figure 1). While it was not possible to doubly deprotonate and alkylate the 4,4′dimethyl-2,2′-bipyridine precursor in a single step, a sequential reaction in the same reaction mixture ("one-pot") could be achieved. The ruthenium complexes were prepared employing microwave techniques, and the complexes obtained were isolated and purified through standard procedures. The structure of the ligands was selected by adopting $[Ru(bpy)_3]^{2+}(PF_6^-)_2$ as a model compound and modifying it in two ways: first, with the addition of long aliphatic chains as in ligand **1**, as well as the nonsymmetric methyl substitution in $[Ru(m\text{-}bpy)_3]^{2+}$ and the bulky *tert*-butyl substituents in $[Ru(dtb\text{-}bpy)_3]^{2+}$ and, second, with the substitution of the dipyridyl framework with the more conjugated phenanthroline ligand.

Electrochemistry and Spectroscopy. The electrochemical properties of $[Ru(bpy)_2(\mathbf{1})]^{2+}(PF_6^-)_2$, $[Ru(\mathbf{1})_3]^{2+}(PF_6^-)_2$, $[Ru(m\text{-}bpy)_3]^{2+}(PF_6^-)_2$, $[Ru(dtb\text{-}dpy)_3]^{2+}(PF_6^-)_2$, and $[Ru(phen)_3]^{2+}(PF_6^-)_2$ were investigated in acetonitrile using cyclic voltammetry, and the results were compared to that of $[Ru(bpy)_3]^{2+}(PF_6^-)_2$. All voltammograms exhibited a reversible wave around +1.3 V, which was assigned to a metal centered Ru(II)/Ru(III) process. In addition, there were three redox waves at potentials below −1.3 V attributed to ligand based processes (Table 1). The effect of the alkyl substituents on the redox potentials was consistent with results obtained from the corresponding methyl substituted complexes.[27]

Table 2 summarizes the UV−vis absorbance and PL properties of the studied Ru complexes. It is apparent that alkyl substituents connected to the 2,2′-bipyridine ligand at the 4,4′-position do not significantly change the UV−vis or the PL characteristics of these materials. However, the small changes in the positions of the metal-to-ligand charge transfer (MLCT) transition and the PL maxima can be correlated to the measured redox potentials. In analogy to many trisdiimine ruthenium complexes, the energy of the absorption and PL maxima of the MLCT transition exhibited a linear relationship with the energy difference between the first reduction and oxidation processes.[30] It is also worth mentioning that the PL efficiency decreased with the number of attached alkyl groups. The PL spectra of the films were found to be very similar to the solution PL spectra. Figure 2 depicts the UV−vis absorbance and the PL spectrum of $[Ru(\mathbf{1})_3]^{2+}(PF_6^-)_2$ in solution as well as the PL spectrum of a spin-coated film as a representative example of the spectroscopic behavior of the studied ruthenium chromophores. Unfortunately, the direct measurement of the PL efficiency in the solid state was precluded by experimental limitations. The results of the spectroscopic studies are presented in Table 2.

Device Characteristics. Typical characteristics are shown in Figure 3 for the $[Ru(bpy)_3]^{2+}(PF_6^-)_2$ device. Upon application of a voltage, the current rapidly increases to its steady-state value. The radiance initially follows the current but then decays exponentially with time. As a result, the external quantum efficiency exhibits the same behavior (Figure 4). These data are in agreement with previous studies of $[Ru(bpy)_3]^{2+}(PF_6^-)_2$ devices utilizing ITO and Al cathodes.[10] Similar characteristics were obtained from the devices of all the other compounds, with the exception of $[Ru(\mathbf{1})_3]^{2+}(PF_6^-)_2$, for which we were unable to obtain a working device. Repeated attempts led to devices that were consistently short-circuited. We suspect that this is due to the low glass transition temperature of this compound, which resulted in failure of the device as soon as a voltage was applied across it.

The current−voltage characteristics from all devices were found to be symmetric with respect to the injecting electrode; that is, they did not exhibit any rectification. This is shown in Figure 4, where the temporal evolution of the current and the radiance from three $[Ru(bpy)_2(\mathbf{1})]^{2+}(PF_6^-)_2$ devices fabricated on the same ITO substrate are displayed. Two were run under forward bias, and their characteristics are shown here to display the device-to-device reproducibility. The third one was run under reverse bias and is shown to exhibit virtually identical characteristics with those of the other two. The efficiency in single layer organic light emitting devices (OLEDs) is determined by the injection of the minority carrier (the carrier that is injected with the lowest efficiency).[31] The fact that both the current and the radiance are the same and independent of bias (despite the fact that we use different electrodes) provides strong and compelling evidence that both contacts are ohmic for both electron and hole injection. This behavior is understandable on the basis of the device operation mechanism, which is dominated by the accumulation of the PF_6^- counterions near the anode and the corresponding depletion of PF_6^- near the cathode. The strong electric field due to the excess negative (positive) ionic

(31) Malliaras, G. G.; Scott, J. C. *J. Appl. Phys.* **1998**, *83*, 5399.

Table 1. Formal Potentials ($E^{0'}$) and Potential Differences (ΔE_P) vs Ag/AgCl in the Ru Complexes Obtained from the Cyclic Voltammograms at 100 mV s^{-1} for a Pt Electrode in Contact with a 0.10 M TBAH/AN Solution Containing 0.2 mM Ruthenium Complex

compound	Ru^{2+}/Ru^{3+} $E^{0'}$ (V) [ΔE_p (mV)]	Ligand/Ligand$^-$ $E^{0'}$ (V) [ΔE_p (mV)]		
		1	2	3
$[Ru(bpy)_3]^{2+}(PF_6^-)_2$	1.34 [79]	−1.28 [61]	−1.45 [70]	−1.68 [69]
$[Ru(\mathbf{1})(bpy)_2]^{2+}(PF_6^-)_2$	1.29 [80]	−1.30 [66]	−1.49 [63]	−1.75 [74]
$[Ru(\mathbf{1})_3]^{2+}(PF_6^-)_2$	1.18 [81]	−1.38 [71]	−1.56 [71]	−1.80 [90]
$[Ru(m\text{-}bpy)_3]^{2+}(PF_6^-)_2$	1.24 [71]	−1.33 [66]	−1.50 [66]	−1.74 [96]
$[Ru(dtb\text{-}bpy)_3]^{2+}(PF_6^-)_2$	1.18 [99]	−1.36 [72]	−1.57 [74]	−1.82 [75]
$[Ru(phen)_3]^{2+}(PF_6^-)_2$	1.21	−1.39	−1.53	−1.84

Table 2. UV−vis Absorbance and PL Properties of the Studied Complexes

compound	absorbance maximum (nm)	absorbance intensity ($M^{-1}cm^{-1}$)	PL maximum (nm)	PL efficiency (%)
$[Ru(bpy)_3]^{2+}(PF_6^-)_2$	451	15 050	605	6.1
$[Ru(\mathbf{1})(bpy)_2]^{2+}(PF_6^-)_2$	454	15 000	612	4.8
$[Ru(\mathbf{1})_3]^{2+}(PF_6^-)_2$	460	15 400	613	4.2
$[Ru(m\text{-}bpy)_3]^{2+}(PF_6^-)_2$	454	15 500	609	4.9
$[Ru(dtb\text{-}bpy)_3]^{2+}(PF_6^-)_2$	459	15 300	610	4.9
$[Ru(phen)_3]^{2+}(PF_6^-)_2$	447	23 000	589	3.3

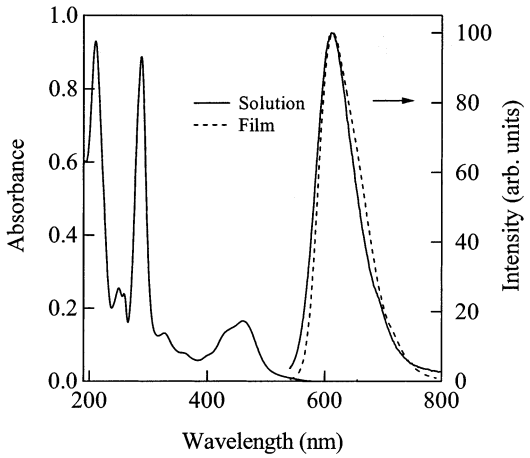

Figure 2. UV−vis absorption and PL properties of $[Ru(\mathbf{1})_3]^{2+}(PF_6^-)_2$.

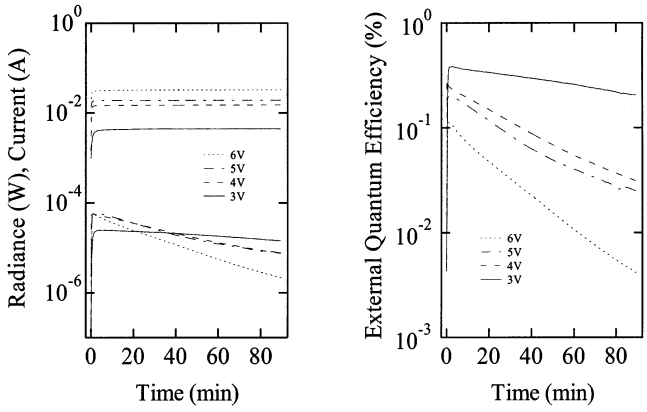

Figure 3. Left: Temporal evolution of the current (top set of curves) and radiance (bottom set of curves) of ITO/$[Ru(bpy)_3]^{2+}(PF_6^-)_2$/Au devices at various voltages. Right: Temporal evolution of the external quantum efficiency of these devices.

charge near the anode (cathode) makes the contact ohmic for hole (electron) injection, regardless of the electrode work function.

The EL spectra were found to be similar to the film PL spectra, exhibiting a small red shift for the two compounds that lack aliphatic side chains. The maxima of the EL spectra are

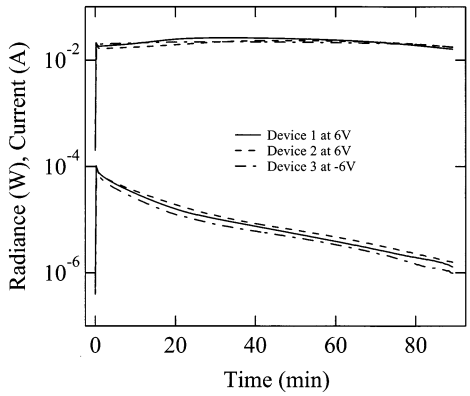

Figure 4. Temporal evolution of the current (top set of curves) and radiance (bottom set of curves) of ITO/$[Ru(bpy)_2(\mathbf{1})]^{2+}(PF_6^-)_2$/Au devices at forward and reverse bias.

Table 3. Device Characteristics of the Ru Complexes

compound	EL maximum (nm)	quantum efficiency at 3V (%)	estimated PL efficiency in film (%)
$[Ru(bpy)_3]^{2+}(PF_6^-)_2$	609	0.5	2.2
$[Ru(\mathbf{1})(bpy)_2]^{2+}(PF_6^-)_2$	612	0.5	2.2
$[Ru(\mathbf{1})_3]^{2+}(PF_6^-)_2$			
$[Ru(m\text{-}bpy)_3]^{2+}(PF_6^-)_2$	612	0.25	1.1
$[Ru(dtb\text{-}bpy)_3]^{2+}(PF_6^-)_2$	611	0.75	3.4
$[Ru(phen)_3]^{2+}(PF_6^-)_2$	600	0.25	1.1

shown in Table 3. The external EL efficiency η of an OLED is given by[26]

$$\eta = b\varphi/2n^2 \qquad (1)$$

where b is the recombination efficiency (equal to 1 for two ohmic contacts[31]), φ is the fraction of excitons that decay radiatively, and n is the refractive index of the glass substrate (the factor $1/2n^2$ accounts for the coupling of light out of the device), which is equal to 1.5. Since emission in these materials arises from the triplet state and singlet excitons are efficiently converted to triplets,[30] the solid-state PL efficiency should be equal to φ and can be calculated from eq 1. The calculated values for all the complexes are shown in Table 3. One should keep in mind that this treatment underestimates the PL efficiencies, since eq 1 does not take into account certain detrimental effects such as quenching of excitons near the metal contacts. As a result, the values reported below represent an upper limit for the solid-state PL efficiencies.

Comparison of the PL efficiencies in solution and in films shows that some degree of self-quenching of the luminescence takes place in these materials, although not to a large degree. As a point of comparison, the PL yield for $[Ru(bpy)_3]^{2+}(PF_6^-)_2$ is reduced by a factor of 2.8, from 6.1% in the acetonitrile

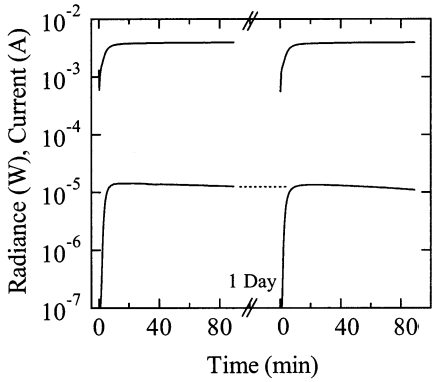

Figure 5. Temporal evolution of the current (top set of curves) and radiance (bottom set of curves) of an ITO/$[Ru(m\text{-}bpy)_3]^{2+}(PF_6^-)_2$/Au device at a voltage of 3 V. The dashed line is at a constant radiance and is only meant as a guide to the eye.

solution to 2.2% in the film. The addition of di-*n*-pentyl and di-*tert*-butyl side chains to the ligand(s) appears to have a beneficial effect in preventing PL self-quenching, as these two materials exhibited the smallest difference between solution and film PL efficiency (less than a factor of 2 for the latter). Overall, these devices operate fairly close to their theoretical limit, with their EL efficiency dictated by the PL efficiency of the films. The latter does not vary dramatically with the ligand substitutions explored here. The highest EL efficiency was observed for the complex with the di-*tert*-butyl side chains (1.5 times higher than that of the $[Ru(bpy)_3]^{2+}(PF_6^-)_2$). An EL improvement with the addition of di-*tert*-butyl side chains was first reported by the MIT group.[19]

To fabricate devices with a higher EL efficiency from these materials, the degree of self-quenching should be reduced. Such a reduction was recently achieved by the addition of small amounts of PMMA in the Ru complexes. $[Ru(bpy)_3]^{2+}(PF_6^-)_2$ devices with an external EL efficiency of 2.7% (which, from eq 1, corresponds to a solid-state PL efficiency of 12.2%) were achieved.[19] It should be noted that the mixing with PMMA seems to be highly beneficial for the photoluminescence, as the PL efficiency of $[Ru(bpy)_3]^{2+}(PF_6^-)_2$:PMMA films is estimated to be twice as high as that in acetonitrile solution. Alternatively, dye doping can be used, where the excitons are channeled to a dye that emits with a higher efficiency.[32−34] We are currently exploring dye doping in these materials.

(32) Suzuki, H.; Meyer, H.; Simmerer, J.; Yang, J.; Haarer, D. *Adv. Mater*. **1993**, *10*, 743.
(33) Kido, J.; Hongawa, K.; Okuyama, K.; Nagai, K. *J. Appl. Phys*. **1994**, *64*, 815.
(34) Wu, C. C.; Sturm, J. C.; Register, R. A.; Thompson, M. E. *Appl. Phys. Lett*. **1996**, *69*, 3117.

Finally, a comment on the stability of these devices is in order. Since air stable electrodes were used and since the same decay in the device efficiency was observed regardless of bias (Figure 4), the origin of this decay must be associated with the degradation of the ruthenium complexes. Since this degradation is more apparent in the radiance, while the current remains constant with time, it is likely associated with a reduction in the PL efficiency, which takes place without affecting, in any major way, the transport properties of the film or charge injection from the electrodes. This degradation was found to be permanent. The radiance of the devices that were switched off, left to rest for a day, and then switched back on again was only as high as that at the end of the first run (Figure 5). However, the degradation was dramatically slowed at low voltages, suggesting that it is current induced. These results are in agreement with literature reports.[10] It should be mentioned that pulsed driving schemes can be used to mitigate this degradation.[18,19]

Conclusions

In conclusion, we have synthesized a family of ruthenium diimine complexes and studied their electrochemical, spectroscopic, and electroluminescent properties. The performance of their electroluminescent devices was dominated by ionic space charge effects. Indium tin oxide (ITO) and gold were found to form ohmic contacts for both hole and electron injection. As a result, their EL efficiency was limited by the photoluminescence efficiency of the ruthenium complexes. The upper limit for the degree of luminescence self-quenching was estimated and found to be relatively small. The di-*n*-pentyl and di-*tert*-butyl side chains were found to be the most beneficial modifications to the dipyridyl ligand in terms of minimizing self-quenching and enhancing device characteristics. Finally, the main degradation mode of Ru(II) devices with air stable electrodes involves the reduction of the PL efficiency of the compounds rather than the degradation of their transport properties or of the charge injection from the metal electrodes.

Acknowledgment. This work was supported by the Cornell Center for Materials Research (CCMR), a Materials Research Science and Engineering Center of the National Science Foundation (DMR-9632275), and by the National Science Foundation (Career Award DMR-0094047). S.B. acknowledges a Fellowship for Advanced Researchers from the Swiss National Science Foundation (Grant 8220-053387). Thanks are due to J.C. Scott for fruitful discussions.

JA0270524